

# Coupled simulation of thermally active building systems to support a digital twin

G.P. Lydon <sup>a,b,\*</sup>, S. Caranovic <sup>a</sup>, I. Hischier <sup>a</sup>, A. Schlueter <sup>a,b</sup>

<sup>a</sup> Architecture and Building Systems, Institute of Technology in Architecture, ETH Zurich, Stefano-Francini-Platz 1, CH-8093, Switzerland

<sup>b</sup> NCCR Digital Fabrication, ETH Zurich, Stefano-Francini-Platz 1, CH-8093, Switzerland



## ARTICLE INFO

### Article history:

Received 15 February 2019

Revised 17 June 2019

Accepted 8 July 2019

Available online 8 August 2019

### Keywords:

Early integrated design

Building simulation

Improved lifecycle energy

Thermally activated building system (TABS)

Digital twin

Digital fabrication

## ABSTRACT

Based on 2050 Swiss and European Union targets, significant energy performance improvements will be required for new and renovated buildings. However, the construction industry has a poor record for delivering productivity and efficiency advancement. As proven in other industries, digital methods can shorten product development time and cost by reducing prototyping with the use of numerical simulation. Further, a digital twin is an extensive computational model of a product that is planned to improve over its lifecycle by leveraging operational data. This paper presents a coupled simulation for the thermal design of a heating and cooling system that is integrated with a lightweight roof structure. The concrete roof structure is shape optimised to provide a low embodied energy building element, which is thermally activated to supply space conditioning from a renewable geothermal source. This work is focused on the modelling methodology used by the energy domain to support the development of a digital twin for a multifunctional building element. High-resolution analysis is used to resolve building physics issues and to provide the initial system performance. A parametric geometry model is used to apply the hydronic pipework to a complex roof shape. With input from the previous two steps, a reduced resolution method is used to add the characteristics of the system to an industry standard whole building simulation model. This final step allows for the development of initial control strategies for the novel multifunctional element. The implications of the research findings are discussed in the context of possible alternations to the building design process due to the influence of digital fabrication.

© 2019 The Authors. Published by Elsevier B.V.  
This is an open access article under the CC BY-NC-ND license.  
(<http://creativecommons.org/licenses/by-nc-nd/4.0/>)

## 1. Introduction

Traditionally, building engineers have largely relied on a sequential approach based on design tables and guidelines. While this approach can be effective, it can also lead to buildings that are overdesigned due to an accumulation of safety factors [1]. Sustainable development has become a prominent societal goal due to concerns by environmental scientists on the shortage of natural resources and the effects that our existence is having on the global environment [2,3]. These concerns have been translated into the 2050 Swiss and European Union energy targets [4], which will require significant energy efficiency improvements for new and renovated buildings.

One method of incorporating sustainable development is to use digital design and to encourage interdisciplinary outcomes [5]. Since the early 1990's, this factor has seen an increase in research in the AEC (Architecture, Engineering and Construction) industry with major improvements in terms of 3D visualisation [6], drawing systems [7], project management [8] and engineering design tools [9,10]. The emergence of digital fabrication has further strengthened the call on the construction industry to utilise digital methods for productivity and efficiency improvements [11]. Barriers to digitisation in AEC are well defined, software cost and expert user time are examples. This work examines the use of application scripting and analysis process automation to demonstrate a viable use of digital methods for the development of a multifunctional building element [12].

Increasing digitalisation at each phase of the construction process has the potential to improve productivity and lifecycle energy performance [11]. Advanced structural design offers a promising pathway to low embodied energy buildings [13]. However within

\* Corresponding author at: Architecture and Building Systems, Institute of Technology in Architecture, ETH Zurich, Stefano-Francini-Platz 1, CH-8093, Switzerland.

E-mail address: [lydon@arch.ethz.ch](mailto:lydon@arch.ethz.ch) (G.P. Lydon).

the energy domain, new structural elements require novel methods for dealing with complex geometry, building physics and operational energy performance issues. If these issues are not adequately resolved, the overall product development process can stall. Therefore, the approach is to provide high-resolution numerical energy analysis to support key areas of the product development. This aids the design of products with non-typical composition or geometry. The overall aim is to build a simulation work-flow for the product development, which can be refined and automated during the manufacturing phase.

In previous work, we presented a CFD (computational fluid dynamics) methodology for the modelling of a lightweight thermally activated building system (TABS) that included a technique for dealing with the complex geometrical and structural constraints [14]. We supplemented the systems model with a CFD comfort model of the associated conditioned room [15]. Further, we detailed the energy analysis of a building at the design phase on a building-scale and a district-scale [12].

The contribution of this work relates to the development of thermal systems for lightweight structures. As the operational behaviour of lightweight TABS can differ from traditional heavyweight TABS, the work is focused on simulation methods for the design phase and the operation phase of a building project. High-resolution analysis is used to resolve building physics issues and to provide the initial system performance. A parametric geometry model is used to apply the hydronic pipework to a complex roof shape. With input from the previous two steps, a reduced resolution method is used to add the characteristics of the system to an industry standard whole building simulation model. This final step allows for the development of initial control strategies for the novel multifunctional element. The solution is formulated based on a digital twin approach with the aim to utilise operational sensor data later in the product lifecycle. The digital twin concept extends a simulation-based systems concept by using the design phase models to support the operation phase with a link to operational data [16].

System integration of sensor and meter data points to the corresponding simulated data is a significant task for the digital twin approach. In addition, the management of simulated and experimental data must be carefully structured to ensure that the active digital twin can be leveraged to efficiently improve future product versions. For this implementation, it was decided that the specification of the simulation methodology would inform the preparation of the system integration planning. Therefore, as the instru-

mentation side specification and testing requires a different skill set, this work will be presented in a future publication.

The paper is organised as follows: to emphasise the contribution of the research, review and background information of relevant topics is outlined in Section 2. Section 3 discusses the methodology for numerical simulation of the multifunctional element. It provides an overview of the modelling specification for the digital twin approach. Sections 4 to 6 outline the results of each simulation component. The value of the methods are highlighted through examples of results, descriptions of the user workflow or the summary of planned or completed experimental validation. Section 7 provides a discussion on the implications of the research outcomes and an outline of future work. Finally, the main conclusions are outlined in Section 8.

## 2. Background and review

### 2.1. Structural design

The Block Research Group (BRG) developed the lightweight thin shell roof, which is based on a lightweight cable-net and fabric formwork system. A numerical method [17] predicts the formwork structural conditions before concrete placement, relative to the final shell shape. This provides a high level of control during the design and construction phases. The structural computational process involves form generation, structural analysis and a multi-criteria shape optimisation. The improvement in structural performance reduces the overall volume of concrete compared to a typical concrete roof section. The shell roof is cast by a reusable and lightweight cable-net and fabric formwork system, which is expected to have less environmental impact compared to a standard method. A full scale prototype of the roof shell, shown in Fig. 1, was completed at the Robotics Fabrication Laboratory at ETH Zurich, Switzerland in 2017.

### 2.2. Embodied energy

The total building lifecycle energy consists of operational and embodied energy. Embodied energy considers the contribution during the construction, demolition and disposal phases (direct), which includes the production of materials (indirect). The operational energy is related to the use of the building, including heating, cooling, lighting and equipment. Embodied energy has traditionally been neglected from the energy analysis of buildings.



**Fig. 1.** Roof shell prototype by BRG (Photo by Michael Lyrenmann).

In the European Union (EU), advances in minimising energy usage have been largely focused on operational energy. Improvements in building envelope performance, energy systems efficiency and on-site power generation are delivering on 2020 targets for Net Zero Energy Buildings (NZEB) [18]. With a view to EU 2050 targets, that is an 80% reduction in greenhouse gas (GHG) emissions from 1990 levels [4], further developments in GHG emissions reduction must also consider the impact of embodied energy.

There is agreement among researchers that the ratio of embodied energy to operational energy cannot be generalised. This is due to the high number of factors involved in the respective calculations, such as climate, geographical location and fuel mix [19]. However, based on studies by Sartori and Hestnes [20] and Bastos et al. [21], it can be agreed that operational energy is typically more dominant in the overall lifecycle. Therefore, when optimising a building element for embodied energy usage, it is important to check the impact of modifications on the operational performance.

The shape optimisation methods outlined in the previous section have the potential to reduce a significant volume of materials. This reduction is related to a specific roof element in comparison to a typical roof element. A detailed embodied energy analysis is outside the scope of this work. However, simplified calculations can provide a guide for the product development. When the structural and operational energy design is at a more advanced phase, a detailed analysis of embodied energy would be beneficial.

### 2.3. Multifunctional element concept

Integrated design improves outcomes of projects requiring cross disciplinary input [22,23]. Due to the large number of dependant factors related to the final metric, this approach is particularly relevant for building lifecycle (BLC) design. The use of multifunctional elements is an application of the integrated design approach. These elements implement a number functions simultaneously by identifying synergies at concept phase [12]. This method is in contrast to sequential design where each element performs a single function.

In addition to structural performance, the lightweight roof integrates a number of other functions. It is a thermally active panel due to an embedded hydronic network (Fig. 2). This feature provides room heating and cooling through the thin concrete radiant panel at ceiling level from a renewable geothermal source. Photovoltaic panels are integrated on the external surface to utilise non-

typical building envelopes as a resource for local renewable energy harvesting during the BLC [24]. Due to the shape and the materials, the roof offers further benefits. For example, thermal mass refers to the use of the internal materials of the building to absorb internal or solar heat gains, this process dampens internal air temperature fluctuations [25].

Integrated design outcomes require additional resources and a higher level of expertise [26]. The implementation of the digital twin concept is planned to distribute the development knowledge over the lifecycle of the product and reduce future design resource requirements. The multifunctional roof element discussed in this paper will be constructed as part of a demonstrator building in Zurich, Switzerland in 2019. See the following Ref. [12] for further information on the building and district scale systems of the NEST HiLo project (Fig. 3).

### 3. Methodology

High-resolution models (Fig. 4a) are used for the initial product development and the exploration of different design strategies. The range of models varies from an edge detail model to a sectional model. As the design starts to mature the sectional model and the complex geometry model are used to provide performance feedback. The complex geometry model (Fig. 4b) takes the actual roof geometry and uses scripting to automate the interaction with the thermal systems. This approach allows the geometry to inform the various simulation models without oversimplification of the connected system and structures. A reduced resolution model (Fig. 4c) is created from the output of the high-resolution sectional model. This allows the roof thermal systems to be connected to a standard whole building simulation model (Fig. 4d). The modelling approach was used to support the product design and to assist with the development of control strategies.

### 4. Results - High-resolution model

In this section, examples of high-resolution analysis related to building physics and TABS performance are presented. This discussion illustrates and highlights the value of this approach for the development of innovative building products. A modelling process automation method, which is solver independent, is also outlined. The commercial CFD code ANSYS Fluent 17.0 [27], based on a control volume approach with the pressure-based solver, was used for

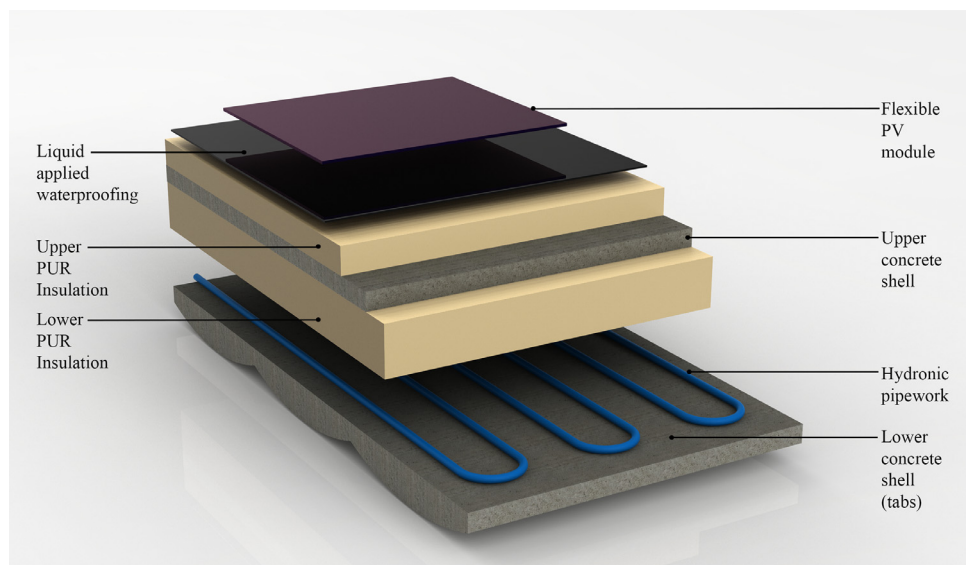


**Fig. 2.** Isometric view of the multifunctional roof element.

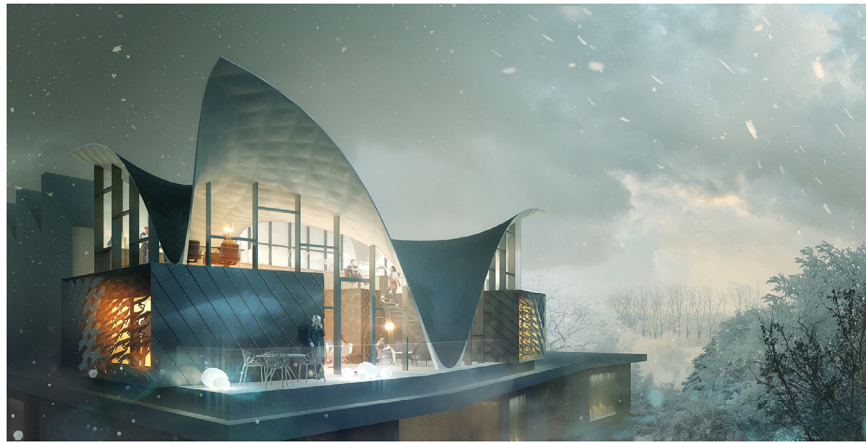


**Fig. 3.** External render of the HiLo building.

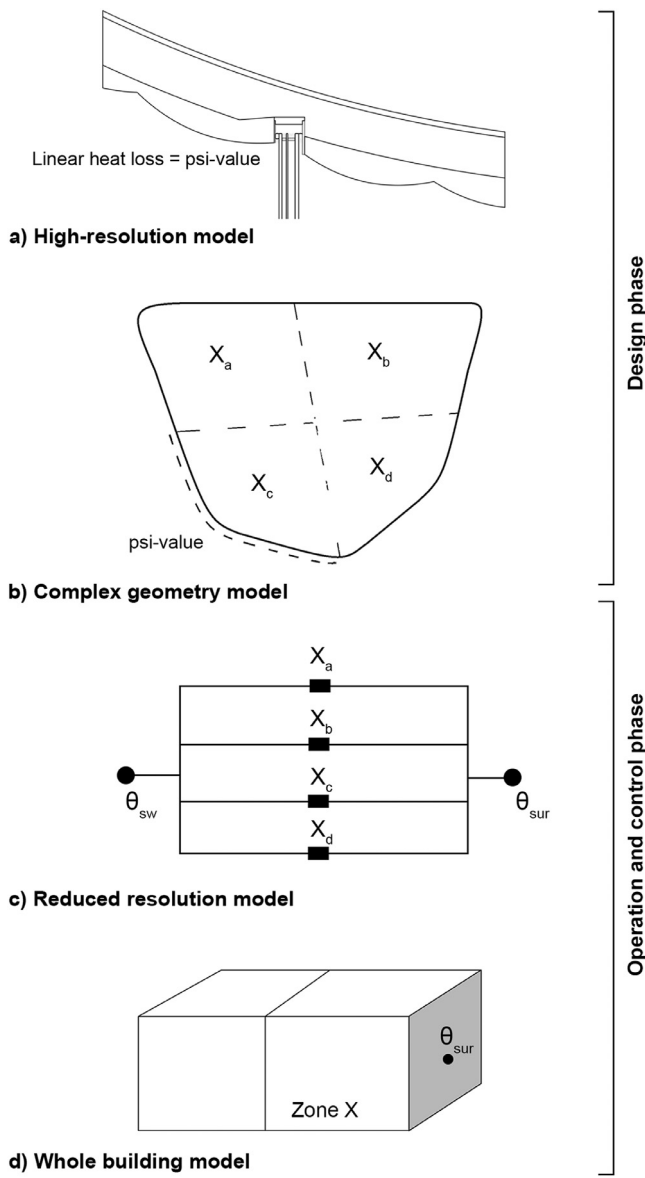


**Fig. 4.** Overview of the modelling methodology over the product lifecycle.

all of the numerical simulations. As the model settings for all of the examples are similar, a single description of model settings is provided in [Section 4.3](#).

#### 4.1. Building physics - Sandwich shell

The design of the multifunctional roof element underwent many design iterations, driven by structural, energy and aesthetic constraints. In terms of thermal performance, the key transition was the change from a single shell to the current sandwich shell. At the roof/facade interface ([Figs. 3 and 5](#)), the lower surface of the shell is exposed internally and externally, which results in a linear heat loss (psi-value) at this interface. This is driven by the total external heat transfer coefficient ( $h_e$ ) of up to 25 W/m<sup>2</sup> K [[28](#)] and the thermal activation of the internal shell. The psi-value at the roof/facade interface was one of the main factors for the development of the sandwich shell.

At an early design stage, a CFD study of the thermal performance of the single shell roof ([Fig. 5](#)) found that the psi-value did not comply with Swiss building standards (SIA 380/1 [[29](#)]). In addition, the thermal losses would have an adverse impact on the performance of the thermally active systems. As the concrete shell is thin (30 to 50 mm) in comparison to a typical concrete roof element (225 mm), commercially available solutions such as thermal breaks or concrete mixes with insulation pearls (expanded polystyrene) could not be easily applied to resolve thermal losses at the roof/facade interface. This issue was further complicated in edge sections by large overhangs that required additional reinforcement for structural performance.

After discussion between the structural and energy teams, the structural engineer proposed a sandwich roof shell [[30](#)], which provided thermally separate internal and external shells. A CFD study of the sandwich shell ([Fig. 6](#)) showed that it had a superior thermal performance compared to the single shell ([Fig. 5](#)) in terms of the psi-value. Further, the preliminary embodied carbon calculations showed that the sandwich shell roof design is superior to a typical concrete roof section in terms of carbon emissions.

To improve the thermal performance, the design roof U-value was set at 0.170 W/m<sup>2</sup> K. This is provided by a lower layer of PU insulation (155 mm) and an upper layer of PU insulation (50 mm) with a thermal conductivity of 0.035 W/m K. At a later stage, further detailing of the sandwich shell facade interface was provided, based on a standard facade detail, as shown in [Fig. 7](#). The analysis results ([Fig. 8](#)) show that the sandwich shell roof complies with the current Swiss energy regulation recommendations.

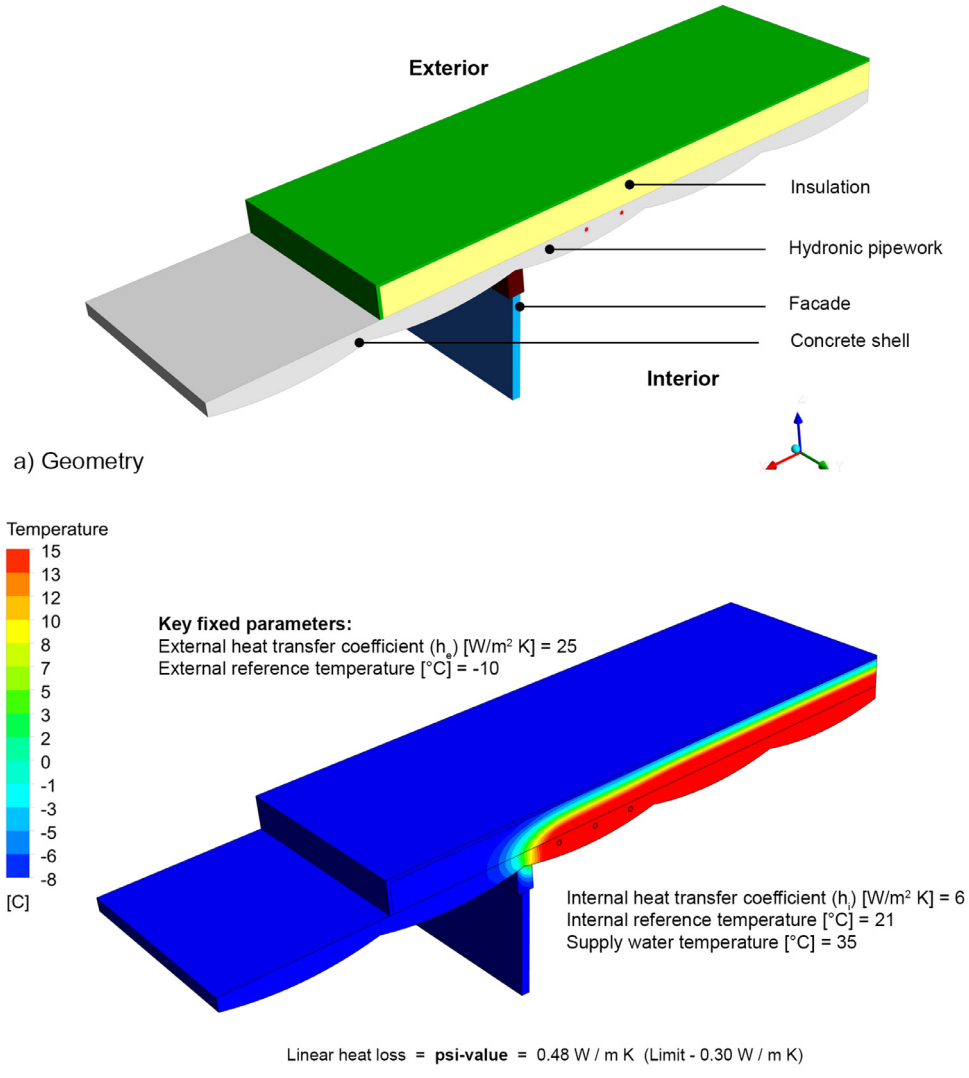


**Fig. 5.** Numerical model results for the single shell roof.

#### 4.2. Building physics - Reinforcement layers and shear connectors

Temperature differences between the external and internal concrete shell volumes would cause stress at the sandwich interface layers. To counteract these forces, it was decided to add shear connections between the shells (Fig. 9a). From the energy perspective, the thermal performance of the TABS panel would be significantly reduced if the shear connection were not planned to consider thermal losses. In addition, the use of reinforcement changes the thermal properties of the concrete panel. This section provides a discussion of the impact of the shear connectors and reinforcement layers on the thermal performance of the concrete panel.

For the roof shell, the three main reinforcing materials options are steel mesh (or fibres), glass fibres and carbon mesh (or fibres). For structural reasons, a carbon fibre mesh was selected as the reinforcing layer and glass fibre reinforced polymer (GFRP) as the shear connectors. A high-resolution model of the roof buildup that included reinforcing mesh layers and shear connections was used to estimate the thermal performance of the TABS panel (Fig. 9). The dimensions of the model were 300 mm (width) x 240 mm (height) x 175 mm (depth). The detailed geometry of the

section resulted in a fine mesh of approximately 8 million cells with hexahedral cells in the fluid domain and tetrahedral cells in the solid domain (Fig. 10). See Section 4.3 for an overview of the procedure for the computational sensitivity analysis. The model included one layer of carbon mesh reinforcement of 1 mm thickness, 12 mm spacing and shear connectors with a cross-sectional area of 30 mm<sup>2</sup>. The thermal conductivity of the carbon reinforcement was set at 16.17 W/m K, the concrete at 1 W/m K and the shear connector at 1 W/m K. A comparison of the temperature contour plots of the reinforced and unreinforced sections, showed that the influence of the reinforcement on the heat distribution was minor.

Fig. 9b shows the temperature contour plots of shear connectors at a central position and located near to the hydronic pipework. Further, Fig. 10 shows the temperature profile along a line on the ceiling surface of the TABS panel. These results show that the shear connectors have a minor localised impact on the panel thermal performance. The local impact is caused by connecting the lower concrete panel to the upper concrete panel by a shear connection (1 W/m K) with a higher thermal conductivity than the lower insulation layer (0.035 W/m K). The additional thermal losses could be offset by increasing the thickness of the upper insulation layer.

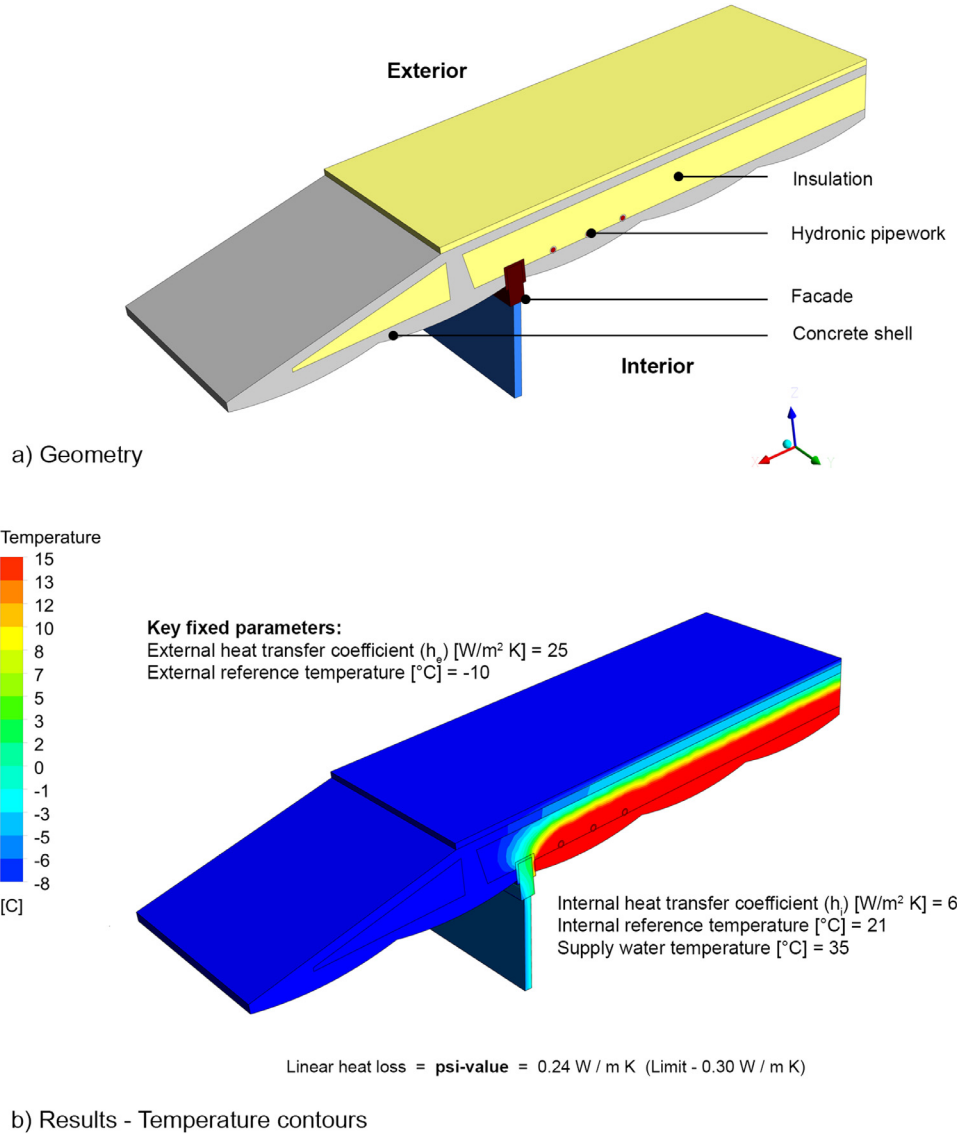


**Fig. 6.** Numerical model results for the sandwich shell roof.

#### 4.3. Performance - Sectional model

After the completion of the building physics models, it was possible to assemble a sectional model that contained the key design parameters of the TABS panel. The results of the building physics models are used to provide a computationally efficient model. For example, the structural reinforcement can be excluded from the geometry as it had a minimal impact on the TABS performance. This model provides the opportunity to modify parameters, such as pipe spacing and insulation thickness, until a suitable level of performance is achieved. Fig. 11a shows the geometry of a version of a sectional model with sample results using a temperature contour plot. An important aspect of high-resolution modelling is to ensure that an adequate computational sensitivity analysis is performed. This section will provide a brief overview of this process.

The heat transfer from the fluid domain to the solid domain was modelled with 3D steady Reynolds-averaged Navier Stokes equations (RANS) CFD simulations with a turbulence model. The performance of the turbulence model requires a suitable mesh resolution depending on the flow velocity and fluid properties. The

numerical performance of a mesh can be estimated by a non-dimensional wall distance value  $y+$ . This provides the size of the first computational cell at the wall of the fluid domain (Fig. 11b). In this case, the performance of the  $k-\epsilon$  model with enhanced wall functions and the Shear-Stress Transport (SST)  $k-\omega$  model will be compared. The latter turbulence model requires a  $y+$  value of less than 1 [27]. Therefore, the SST  $k-\omega$  model requires a significantly larger computational mesh. Fig. 11b shows images of the computational mesh used for the sensitivity analysis. Mesh-03 is used for the SST  $k-\omega$  turbulence model. Mesh-01 and Mesh-02 were used for the  $k-\epsilon$  turbulence model. Each mesh was constructed with hexahedral cells that resulted in a maximum skewness value of less than 0.7 and minimum orthogonal quality value of 0.5. To evaluate the performance, a line (line1) is placed at a location of high temperature gradients. The results in Fig. 11c show that the performance of both turbulence models is similar. As the  $k-\epsilon$  turbulence model requires less computational resources, it was used for the sectional model. It should be noted that geometry of the pipework for the sectional model is relatively simple. In cases that the fluid encounters a more complex geometry or has a higher Reynolds number,

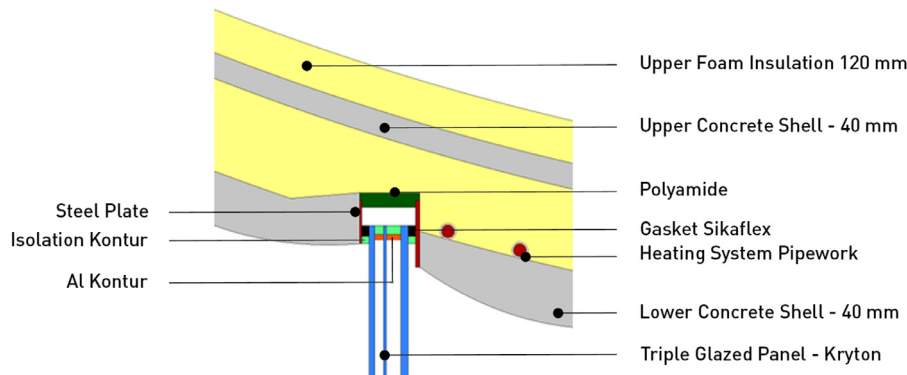


**Fig. 7.** Numerical model geometry for the detailed sandwich shell roof.

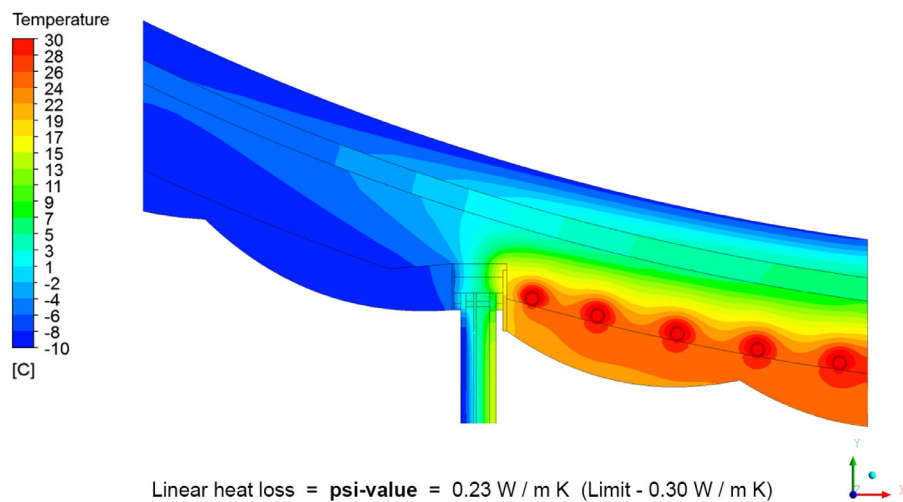


**Fig. 8.** Numerical model results for the detailed sandwich shell roof.

the SST  $k-\omega$  model has been shown to be superior to the  $k-\varepsilon$  model for heat transfer cases [31].

It is also important to ensure that the solid domain has a suitable mesh resolution. Fig. 11b shows images of meshes with a fine (Mesh-03), medium (Mesh-02) and coarse (Mesh-01) resolution. As shown in Fig. 11c Mesh-01 does not capture the correct temperature profile in the concrete solid. Mesh-02 is a good balance between mesh size and accuracy, therefore resolution of Mesh-02 is used for the solid domain. As the complex geometry of the model is mainly related to the solid domain, the computation run time (approximately 7 minutes per case on a 16-core Intel Xeon workstation) is not a barrier to applying CFD analysis within a digital twin.

#### 4.4. Model automation

One of the barriers to high-resolution modelling is the requirement for extensive expert user setup time. While many commercial codes provide methods of automation, these solutions are dependent on the commercial code and can have limitations depending on the user case. In this section, we discuss the use of a solver independent automation process that is customised to the user case. The aim is not to replace the domain expert but instead to reduce the overall setup time. Further, this allows a non-expert user to modify the input parameters to generate useful results. The automation of the case setup and results post-processing is developed using windows based open source scripting methods.

With reference to Fig. 12, the automation process is described below:

1. CFD expert: The first step is to create the computational mesh (.msh) and the model settings (case) file (.jou). The previous two building physics steps are used to inform the mesh and case file creation. Depending on the problem, one or a number of meshes can be included. This step is completed by the CFD expert.
2. Systems expert: When the CFD model has been setup and tested, the expert knowledge and judgement is captured in the case and mesh files [32]. Therefore, it is reasonable to transfer responsibility for the next steps to the systems expert. As the case file is human readable, it is possible for the systems expert to identify the model parameters to be varied. This step is completed by replacing the parameter value with a key word. The updated case file becomes a template, which is used to generate a set of case files in the next step. A range of values is also selected and stored in the parameter list file.
3. Case generator: Python code is used to generate all of the possible combinations based on the parameter values and meshes. These combinations are recorded in the case index file. A Python reader code is then used to build the CFD case files based on the case index.
4. Auto run: All of the case files and mesh files are moved to a folder, which contains a Windows batch (script) file [33]. This script counts the number of case and mesh files. Based,

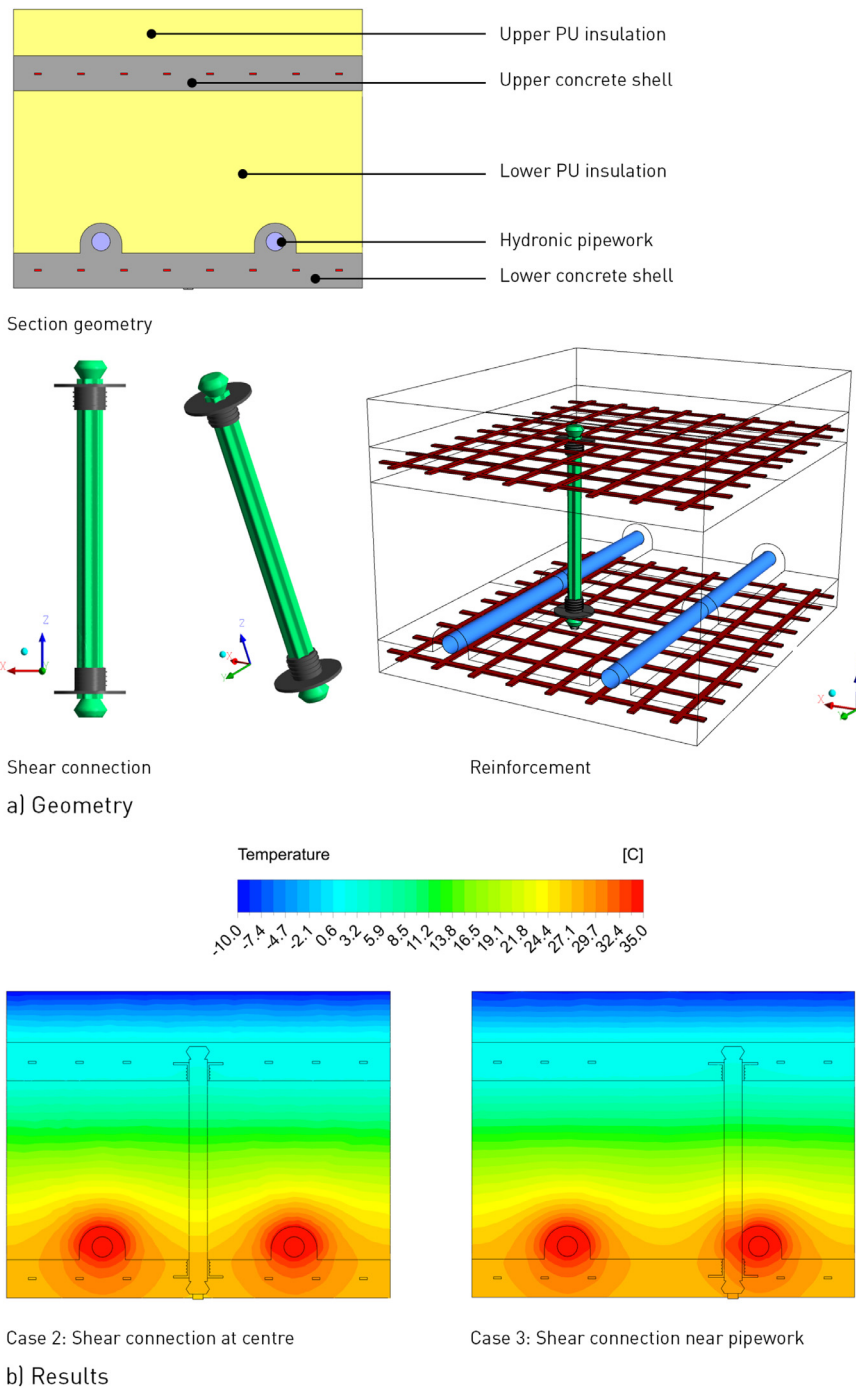


**Fig. 9.** Numerical geometry and results for the shear connectors.

on the file calculation, the folder structure is built and indexed. When the folder structure is complete, the run solver cycles through the case index and transfers the results to the relevant case folder.

5. Post processing: A Python code using Pandas (open source Python library for data structures and data analysis) [34] is then used to extract the results from each folder and transfer to a dataframe. The results dataframe can then be easily modified to visualise the output data.

As described above, the automation process separates the model setup by the CFD engineer from the model running and re-

sults analysis by the systems engineer. For example, the systems engineer can run a set of CFD simulations to compare the impact of varying the properties of the concrete mix on thermal performance. The results can be post-processed without a detailed understanding of the CFD workflow. Therefore, modifications to key components (e.g. the edge detail) can be easily updated and transferred to the whole building model (Fig. 4d). The main limitation of the automation process relates to major changes to the geometry. These changes currently require the intervention of the CFD engineer to create a new mesh and index in the library. This step could also be fully automated. However, the quality of the computational mesh is a vital component in the overall modelling

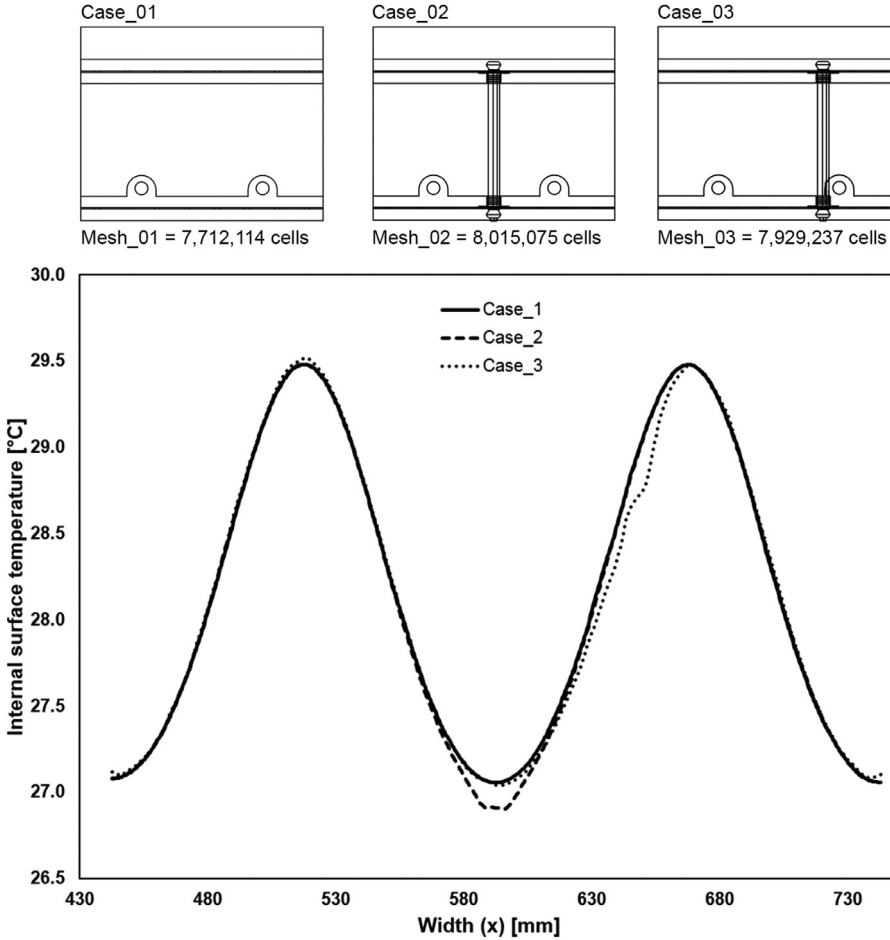


**Fig. 10.** Thermal analysis of the shear connectors - temperature profile on heating surface.

**Table 1**  
Extract from the case\_index.csv file for the heating systems study.

filename	inlet_t	inlet_v	in_ref_t	in_htc	ex_ref_t	ex_htc	pu-lower_lamda
Jou_1.jou	29	0.5	18	6	-8	25	0.035
Jou_2.jou	29	0.5	18	7	-8	25	0.035
Jou_3.jou	29	0.5	18	8	-8	25	0.035
Jou_4.jou	29	0.5	21	6	-8	25	0.035
Jou_5.jou	29	0.5	21	7	-8	25	0.035
Jou_6.jou	29	0.5	21	8	-8	25	0.035
Jou_7.jou	29	0.5	24	6	-8	25	0.035
Jou_8.jou	29	0.5	24	7	-8	25	0.035
Jou_9.jou	29	0.5	24	8	-8	25	0.035
Jou_10.jou	32	0.5	18	6	-8	25	0.035
Jou_11.jou	32	0.5	18	7	-8	25	0.035

framework. Therefore, it is more prudent to retain the CFD expert for this task. The value of this approach has been highlighted in previous research studies [35].

#### 4.5. Sectional model results

This segment presents the results of the sectional model for a heating study. The sectional model has a high number of parameters from the thermal conductivity of the solid materials to the model boundary conditions. All of these parameters are present in the case index file (Fig. 12 and 1). To prepare the set of case (.jou) files for the heating study, the parameters of interest are identi-

fied and this provides a list of variables. For example, the variable parameters for the heating study are supply water temperature (5 variables), internal heat transfer coefficient ( $h_i$ ) (2 variables) and internal reference temperature (3 variables). Based on the overall number of variables, there are 45 possible case combinations. All of the other parameters are fixed, such as external temperature at  $-8^{\circ}\text{C}$  and  $h_e$  at  $25\text{ W/m}^2\text{K}$ . When all of the cases have been solved, the results data is automatically post-processed to provide an estimate of the performance of the TABS panel (Fig. 13). This approach is feasible due to the reduction in expert user time by process automation and by the use of a parallel solver with multi-core processors.

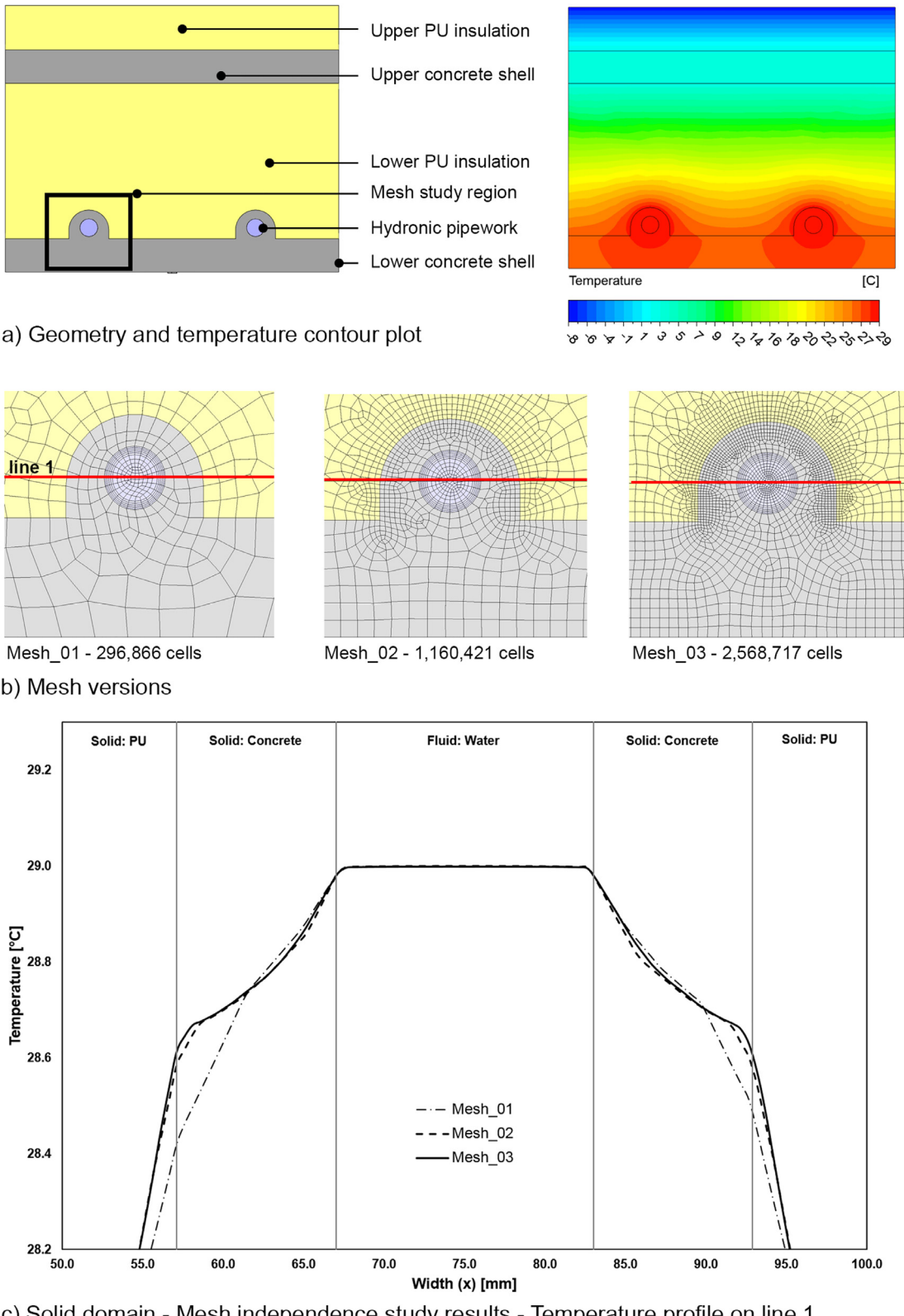


**Fig. 11.** Mesh independence study of the sectional model.

High-resolution models are closely aligned with the physical mechanisms of the studied system. Therefore, the model can be used to solve a range of problems. This is not achieved by modifying the model but by adjusting the extraction of results data and processing to a suitable domain format. For example, the sec-

tional model was envisioned to evaluate the heating and cooling performance of the TABS panel. However, during the design phase the structural engineer requested thermal input on the temperature difference between the upper and lower shells (Section 4.2). This input was created by modifying the results data (Fig. 14).

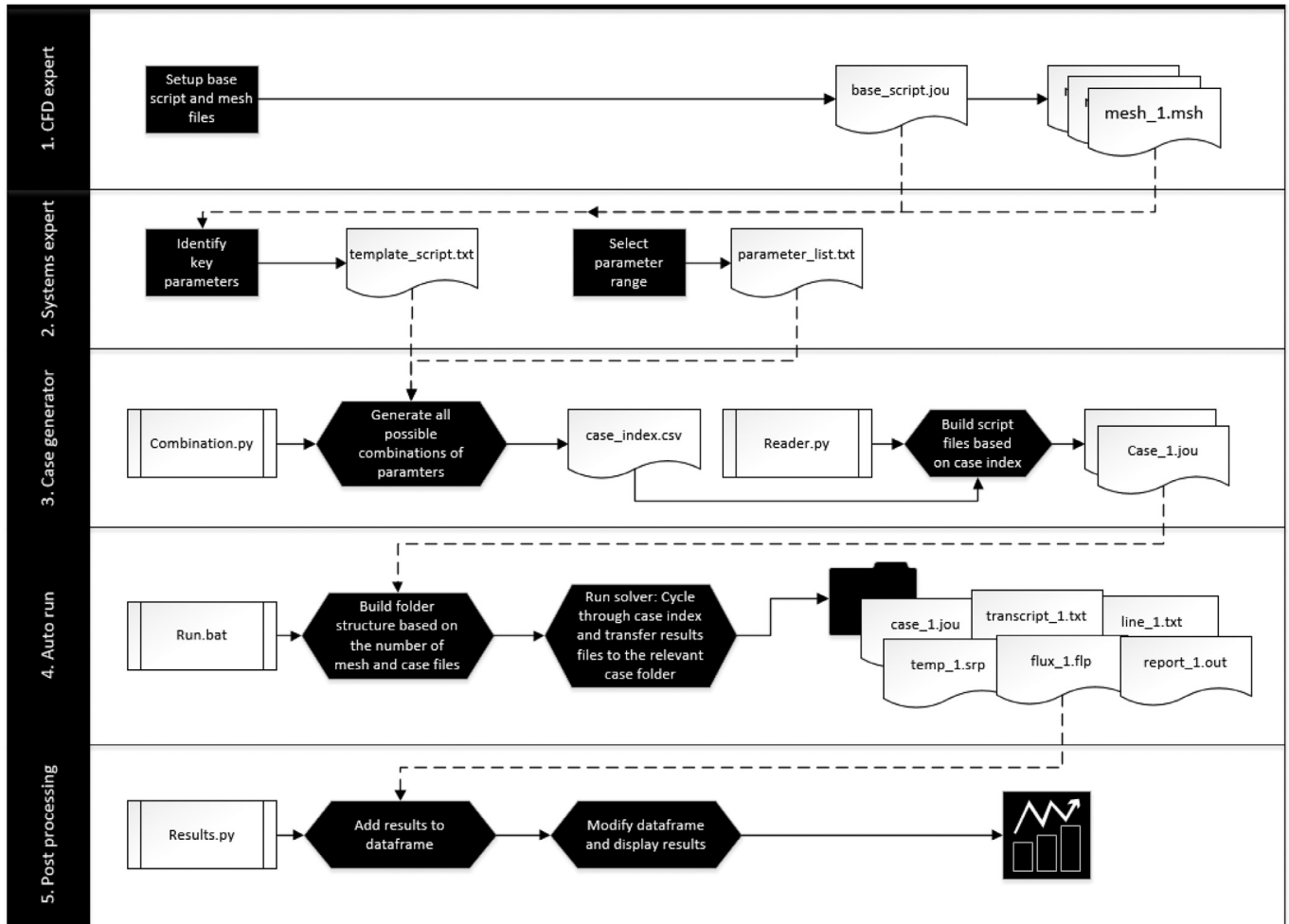


Fig. 12. Overview of the model automation process.

## 5. Results - Complex geometry model

In contrast to other manufacturing industries, geometrical variation is a significant resource sink for the realisation of a building project [36]. This task is a critical interface between the design and the construction phases. The application of the hydronic pipework on the doubly curved geometry of the concrete shell is a useful example of a geometrically complex problem. It can be expected that the geometry will change significantly from project to project and a high level of interdisciplinary interaction will be necessary [14]. A lack of preparation for this task can have a significant impact concerning project time planning, cost and overall product performance. Further, an innovative product involving complex geometry cannot be readily accommodated in standard building information models (BIM) (e.g. IFC or gbXML). Therefore, the provision of digital methods to assist a project planner with this task is essential for the market acceptance of a building product. Based on this requirement, a robust method to support the testing and planning of the hydronic pipework is a key design problem regarding the TABS performance and the final construction process. To support the transition of the research geometrical model to a standard BIM representation, an interdisciplinary online repository will be developed in the COMPAS project [37], which is an open source Python-based computational framework. This work will combine the energy systems, structural and architectural specifications, which can then be translated to a BIM object when the overall lightweight TABS product matures.

In this section, a CAD system [38] with visual programming [39] is used to support the placement of hydronic pipework on a roof geometry. The concept and the user process of the scripting are described to illustrate the functions of the application. In addition, a pipework placement experiment on a 1:1 prototype (Fig. 1) was completed to test the performance of the method.

### 5.1. Model automation

Steps for the selection of hydronic loop fields, pipework generation and anchor point locations:

1. Based on the average pipe spacing from the high-resolution model (Section 4.5) and the total active roof surface, estimate the total pipe length needed.
2. Decide on the number of loop fields to cover the active roof surface.
3. Visually divide the top-view of the roof in convex polygonal fields of similar area and proportions. Preferably, define areas with almost square proportions.
4. Assign numbers to the loop fields, starting with those that have a higher requirement to be of a certain length, or that correspond to areas of large curvature variations (Fig. 15).
5. Draw the control polylines on the two opposite sides that have stronger curved edges (Fig. 16).
6. Draw the boundary polylines (Fig. 16).
7. Set up the Grasshopper script inputs (Fig. 17):

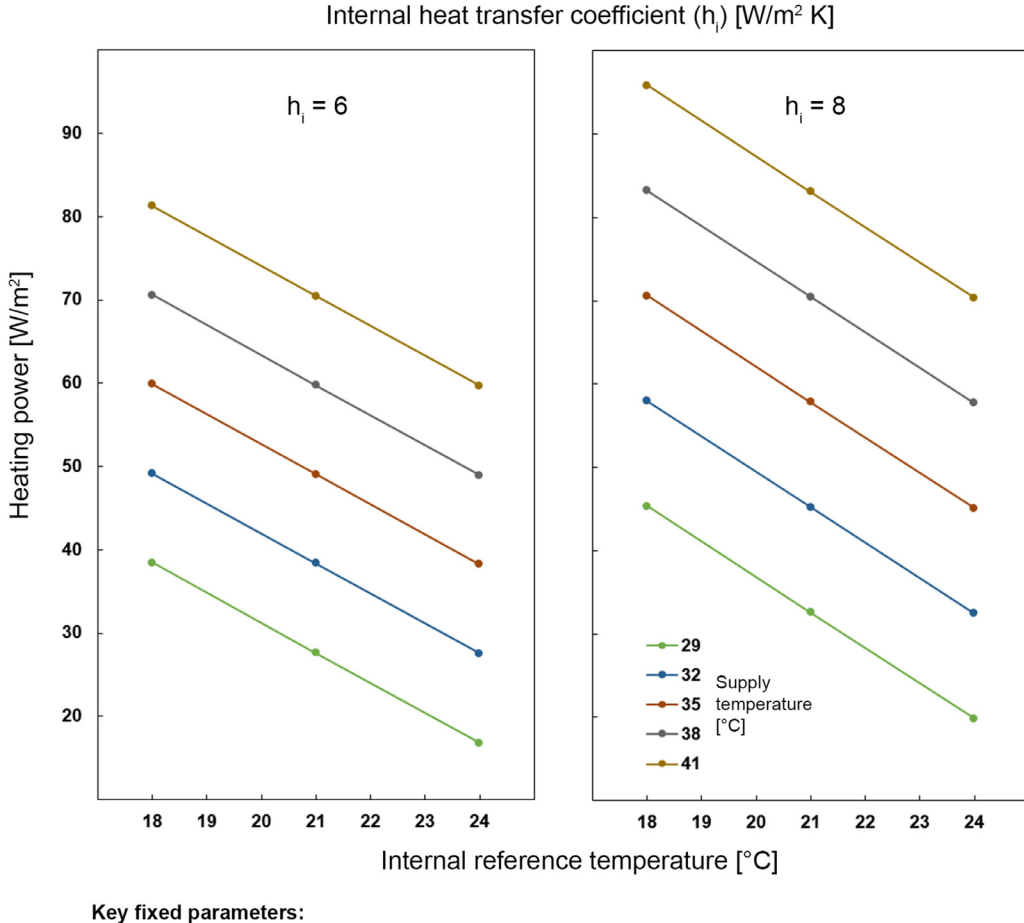


**Fig. 13.** Heating performance of the roof TABS panel.

- (a) Choose the roof mesh, the control polylines and the boundary polylines
- (b) Set the pipe spacing (distance)
- (c) Choose the number of levels for the pipe loop spiral (start with a low count and increase until the field is completely covered, up to the centre)
8. Iterate through multiple input parameters until a satisfactory result is reached for the basic shape of the pipe loop.
9. Once the basic geometry has been found for the pipe loop, update the data dam and go on with the manual adjustments, anchor point avoidance and mounting points generation.
10. Bake the projection of the pipe loop on the XY plane.
11. Manually draw the inlet/outlet extensions and adjust the pipe loop projection as required. Make sure to rebuild the curve with a reasonable number of points in order to avoid having kinks or deviating significantly from the base curve.
12. Import the adjust curve to Grasshopper.
13. Set the distance that the anchor points (shear connectors) should be avoided by (anchor threshold).
14. Set the number of attenuation points, defining how smoothly the anchors will be avoided.
15. Set the distance between the mounting points to be generated.
16. Set the number of field subdivisions for analysing the average inclination.
17. If needed, manually insert additional mounting points using the position slider and the data recorder.

18. After achieving a satisfactory result, bake the geometry of the pipe loop.

## 5.2. Model validation

Fig. 18 shows an image of the final hydronic pipework layout for the HiLo project. The key outputs are updated pipe spacing, loop area, loop surface slope, pipe length for each loop and a list of coordinates for the mounting position for the hydronic pipework.

A 1:1 prototype of the HiLo roof shell was constructed for assembly process and structural testing. This prototype was used to test an early version of the visual programming application. Fig. 19 shows the completed test where pipework loop was planned and the mounting point locations were predicted.

## 6. Reduced resolution and whole building model

### 6.1. Whole building model

The selection of a whole building simulation model is dependent on the project phase. For the HiLo project, the simulation framework for the design phase and the operation phase is shown in Fig. 20. At the design phase a simplified model (Lesosai [40]) is used to facilitate quick annual simulations, which are compliant with Swiss energy regulation. The sacrifice of accuracy for speed is justified due to the high variability of the design parameters during this phase. This design phase model provides feedback to the design team in terms of the performance of the building and district

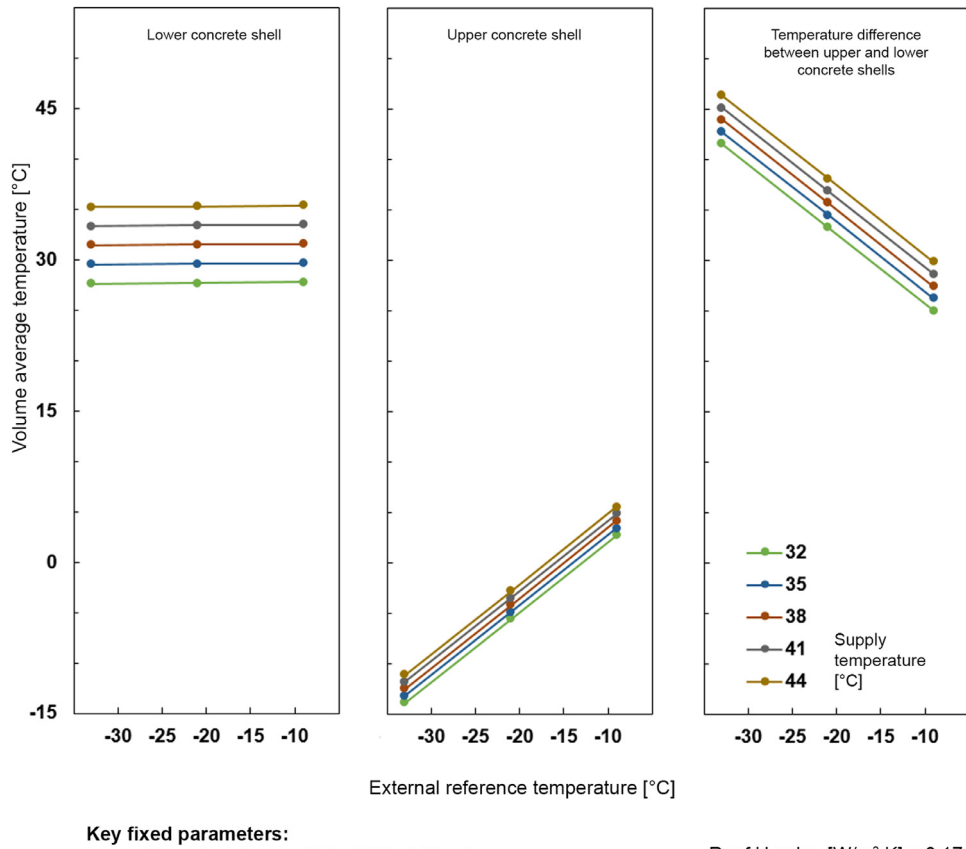


**Fig. 14.** Structural performance study of the temperature difference between the upper and lower concrete shells with a range of supply water temperatures.

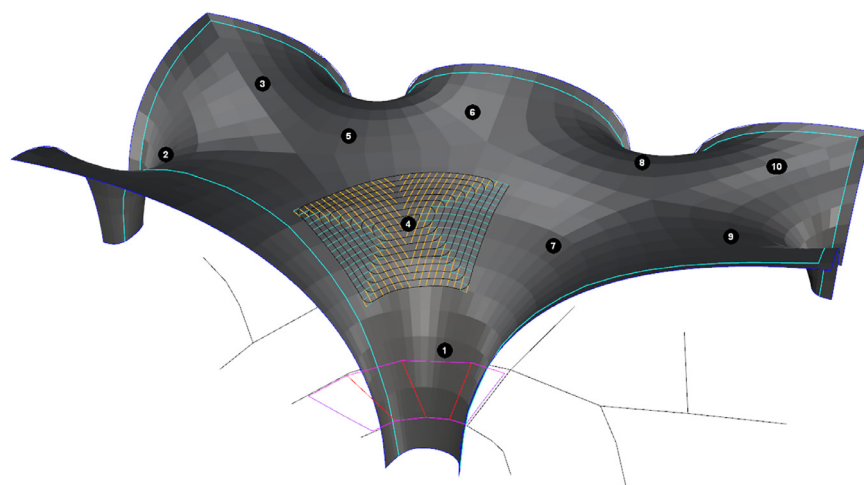


**Fig. 15.** Selection of the loop fields on the roof surface with an assigned index.

systems. For example, the impact of changes to the building layout and facade surface area. As investigated in previous studies, a significant performance gap in comparison to the actual energy usage is expected in these results due to simplified systems and occupant modelling. For more information on the design phase modelling of the HiLo project, see the following Ref. [12].

As the design phase is completed, the main parameters become fixed, such as the building envelope and the sizing of the heating and cooling systems. For the operation phase the focus shifts to the control strategies for the building systems. Therefore, the operation model is initialised with the design phase model using the final

geometry and system sizing results. The simulation period is also reduced to a one month duration to focus on a particular set of conditions. The key feature is that the simulation results can be compared to actual sensor data [41]. This feedback to the model is used to refine and improve the control of the current building systems and the design of future buildings.

The main concept of the operation model is that the core calculations are performed with a whole building simulation model that is suitable for control studies. TRNSYS has been shown to be a robust and adaptive method for modelling thermal energy in buildings [42]. In cases where the operation model does not fully

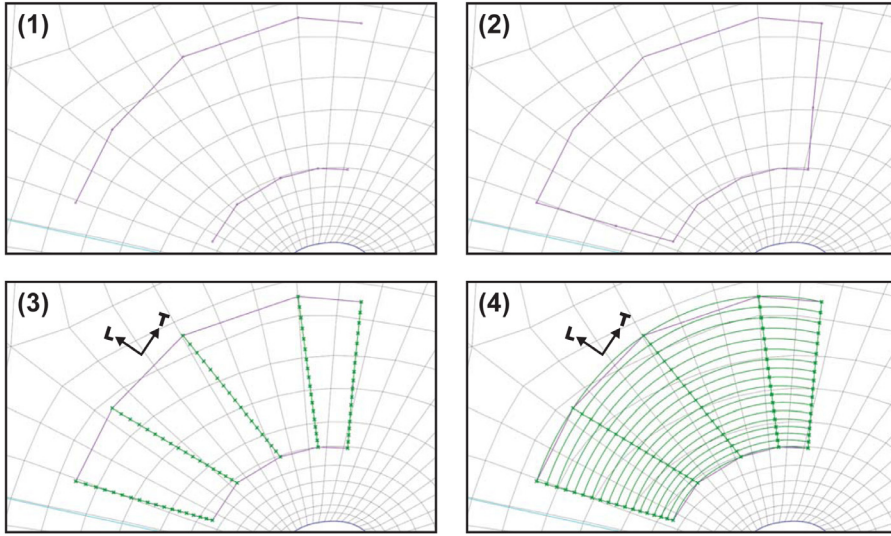


**Fig. 16.** Initial control polylines for a loop field.

capture the complexity of a system, the systems in question are modelled in an external application and the results are transferred back to the operational model. An example of this approach is the TABS model, where MATLAB is used to provide a custom resistance capacitance (RC) model and the output is then transferred to TRNSYS. In addition, the ventilation systems are modelled in CONTAM to fully capture the system complexity. An overview of the whole building simulation model is shown in Fig. 21.

## 6.2. Reduced resolution model

Based on the output from the high-resolution model, a reduced resolution model is created to enable the assessment of TABS performance within a whole building simulation. TRNSYS provides a standard TABS model that has been tested and validated. However, as the roof TABS is still in a development phase, a more detailed model is required. The main function of the TABS reduced resolution model is to capture variations in concrete thickness (30 to 50 mm), surface slope (horizontal to near vertical) over the total surface of the roof TABS. By capturing this additional level of detail, the impact of the variation can be investigated.

Previous work by Gwerder et al. [43] is used as the basis for the reduced resolution model. The key difference is the addition of subdivisions of the model structure. These subdivisions allow for the local variations to be inserted in each hydronic loop of the TABS panel [44].

## 7. Discussion and future work

This section provides a discussion on the implications of the presented modelling methods for design teams and digital fabrication. The discussion is in the context of the design phase of a real building project with a multifunctional building element. In addition, a summary of future work is outlined.

### 7.1. Implications of the digital twin approach for digital fabrication

Accelerating the development timeline was a key driver for the selection of the modelling methodology for the design phase of the novel multifunctional element. These methods can also be applied in general for evaluating and supporting energy related innovation in the built environment. Digital fabrication involving off-site fabrication with the influence of robotics has the potential to change

the limitations and constraints of traditional construction methods by providing adaptable and controllable workflows. For the energy domain, new design methods will have to be adopted to leverage the increased flexibility of digital fabrication. As demonstrated with this work, the digital twin approach can be used to support new methods of construction by evaluating performance in terms of a whole building simulation.

### 7.2. Implications of the digital twin approach for design teams

This work was completed during the design phase of a demonstrator building project. This provided day to day interaction with industry planners and consultants. Based on this experience, it became clear that a significant barrier to digital construction is the current planner workflows for constructing buildings. This process is typically fragmented and sequential, which makes it very difficult to focus on adaptable high performance outcomes. These issues have been highlighted in previous studies. Examples range from low rates of investment in R&D to split incentives relating key energy performance decisions [45,46].

In terms of building design, the approach of combining key attributes into a multifunctional element has a number of advantages. Firstly, an integrated design approach is ingrained from the product concept, which is uncommon in the built environment. Secondly, the overall value of the multifunctional element can be increased in comparison to a sequential construction method by reducing on site construction time with the potential to improve overall performance. This method could encourage a single company to develop and market the element as a self-contained product. A single stakeholder would provide the opportunity to concentrate dependant analysis workflows in one location. This results in the responsibility for the overall product performance to be transferred to a single stakeholder. It implies that the planning and consultant engineer will manage the process of an individual building product by modifying digital twin models supplied by the company. Further, as new products enter the market a selected building could transfer measurement data to drive improvement and acceptance by leveraging the digital twin concept.

### 7.3. Future work

Simulation automation methods are available in most modelling software packages. In this case, a custom automation method was

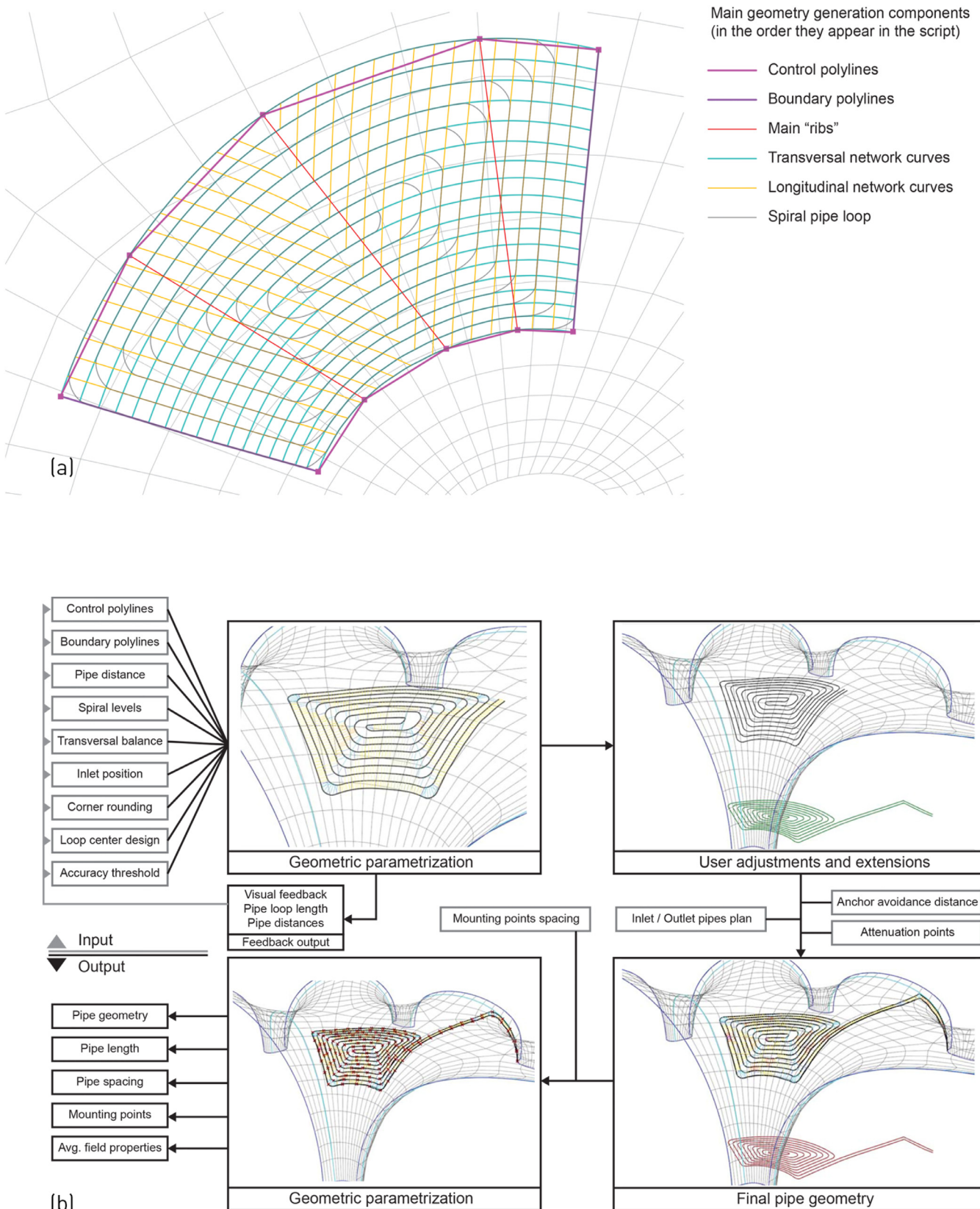


**Fig. 17.** (a) Outline of the main geometrical components. (b) Overview of the script inputs and outputs.

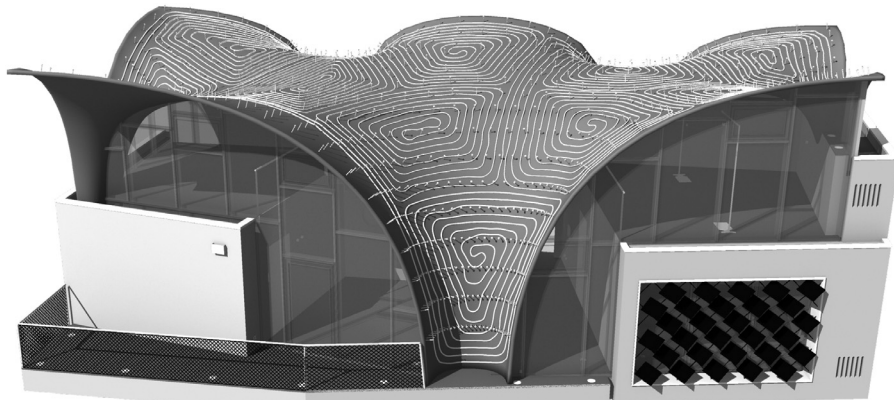


**Fig. 18.** Final layout of the hydronic pipework of the HiLo roof.

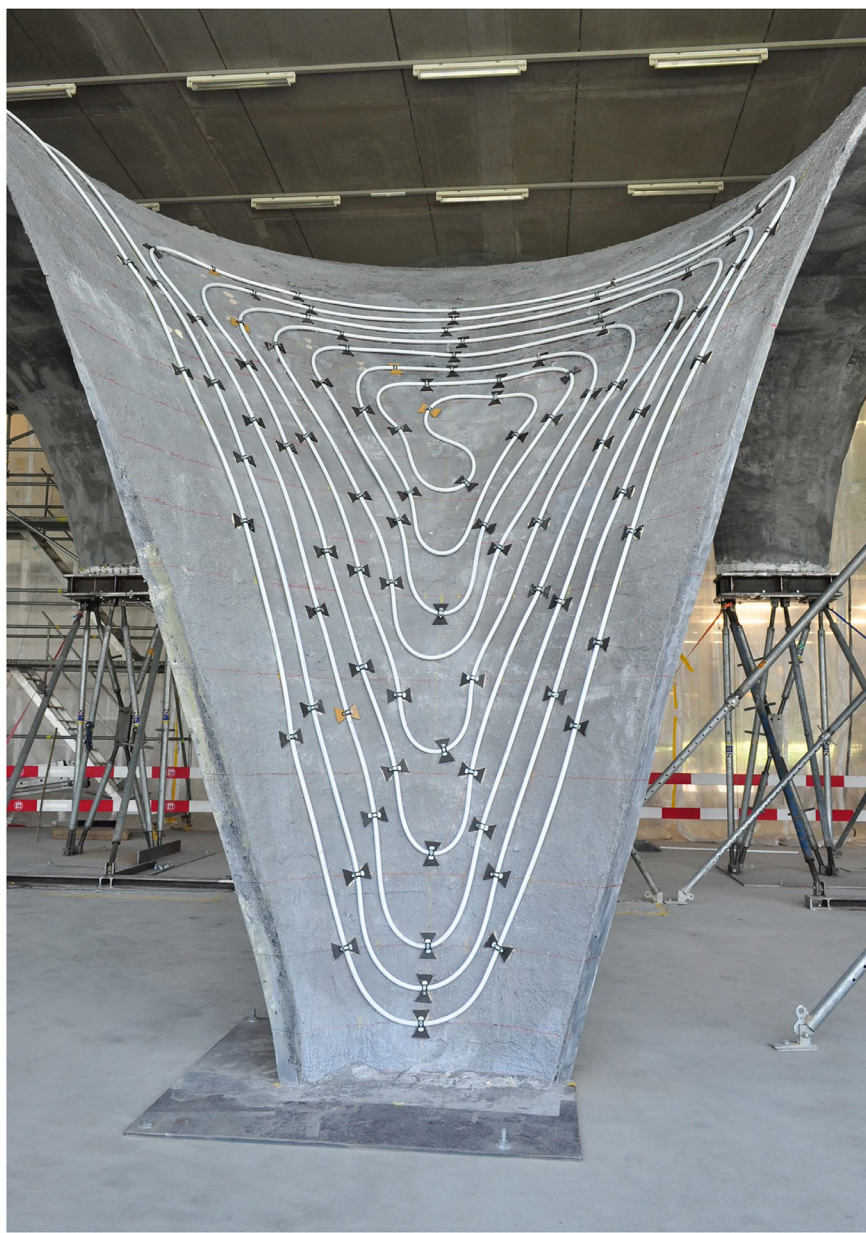


**Fig. 19.** Hydronic pipework experiments of the 1:1 prototype.

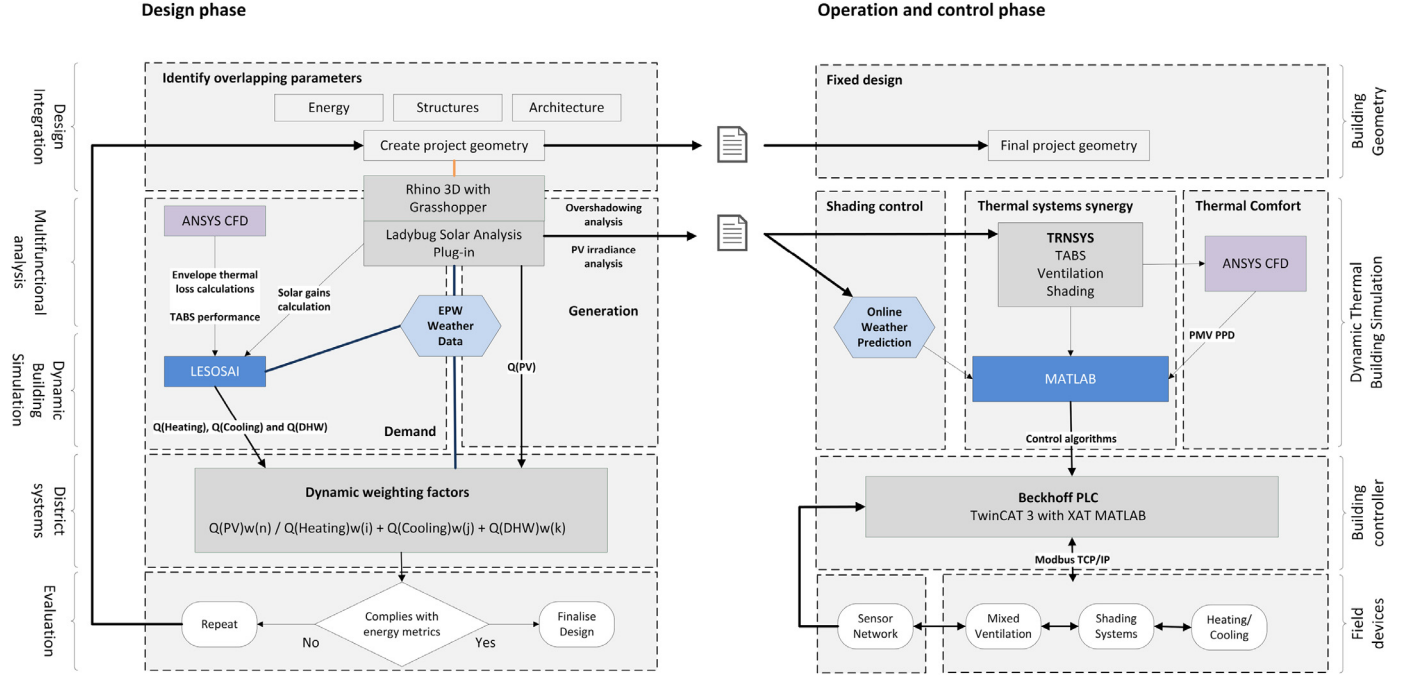
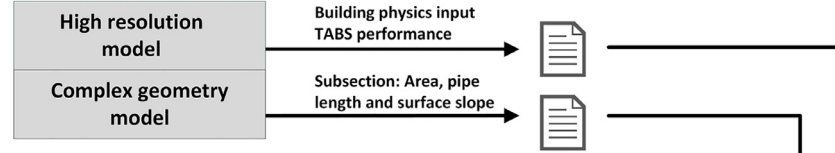


Fig. 20. Whole building simulation (a) Design phase [12] (b) Operation and control.

### TABS initialisation data



### Whole building model

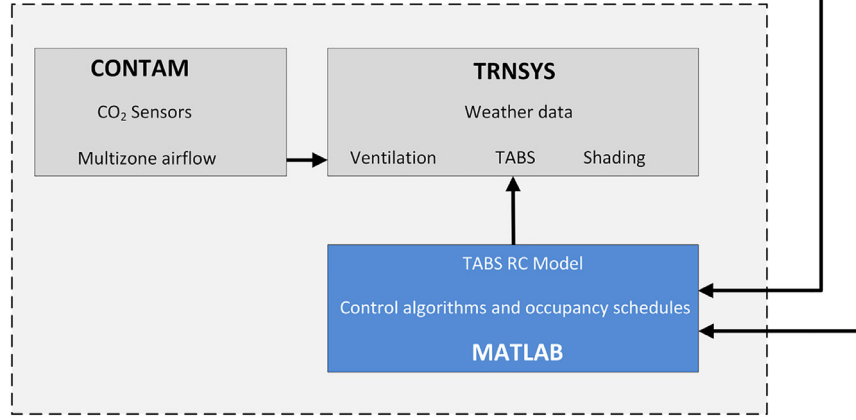


Fig. 21. Whole building simulation – connectivity overview.

developed for a number of reasons. Firstly, the commercial simulation automation had some limitations in terms of results post processing and the possibility to link results with other software. Secondly, it was preferred that the automation method would be application independent. As software cost is a barrier to the adaptation of high-resolution methods, this would allow the replacement of a commercial code with a suitable open source code. An additional driver was the availability of robust, open source and well-documented scripting languages. A notable example is Python with

extension libraries such as Pandas for data structures [34] and Seaborn for data visualisation [47]. Further work is planned on the inclusion of open source tools and solvers.

Computational models should be validated to ensure that the required level of accuracy is delivered. As the TABS setup is novel, there were no available experiments to capture the geometry, materials and systems of the panel. The TABS panels will be constructed in a real building. However, it would be difficult to control the key experimental variables and boundary conditions within the

setting of an operational building. While the real building case is expected to provide valuable results relating the systems performance, it was decided that preconstruction experiments would benefit the product development. Therefore, based on the initial simulation results, a small scale experimental setup will be designed to provide a method of validation for the sectional model. Further, the small scale prototype will support the system integration of sensor and meter data with the simulation structure. The setup includes all of the key system components and sensors of the planned digital twin.

Future simulation work will focus the conditioned zone in terms of thermal and occupant comfort. The planned models will require higher computational resources [15] in comparison to the operation and control models. Therefore, a similar custom automation approach will be followed in order to reduce the CFD expert user time. In addition, it will be essential to plan the simulation process to facilitate the reliable comparisons of simulated and thermal comfort experimental data within the digital twin concept.

## 8. Summary and conclusion

This paper presented simulation methods for the design of a thermal system that is integrated in a lightweight roof structure. The methodologies are based on a digital twin approach with the long term strategy to link simulated and sensor data. It is expected that this will reduce the high planning resources necessary for the implementation of multifunctional building elements. Further, a digital twin approach has the potential to support methods of construction that are related to digital fabrication in general.

High-resolution models were used to resolve building physics and systems performance issues at the development phase. A model automation method, which is solver independent, was implemented to reduce expert user time and to provide controlled access to a non-expert user. A CAD system with visual programming was used to parametrise a complex geometrical task. This involved the planning of hydronic pipework layout and the calculation of the mounting point positions. Finally, the design phase models were extended to provide a whole building simulation model with a focus on the development of the initial control strategies for the multifunctional element.

## Declaration of competing interest

I certify that the authors have NO affiliations with or involvement in any organization or entity with any financial interest (such as honoraria; educational grants; participation in speakers bureaus; membership, employment, consultancies, stock ownership, or other equity interest; and expert testimony or patent-licensing arrangements), or non-financial interest (such as personal or professional relationships, affiliations, knowledge or beliefs) in the subject matter or materials discussed in this manuscript.

## Acknowledgements

D. Thomas from the Architecture and Building Systems Group, ETH Zurich, provided software engineering support for the automation and scripting methods. This research has been partially financially supported by the National Centre of Competence in Research (NCCR) Digital Fabrication, which is funded by the Swiss National Science Foundation and the Commission for Technology and Innovation (CTI) within the Future Energy Efficient Buildings & Districts (SCCER FEEB&D).

## References

- [1] S. Sorrell, Making the link: climate policy and the reform of the UK construction industry, *Energy Policy* 31 (9) (2003) 865–878.
- [2] R. Gasper, A. Blohm, M. Ruth, Social and economic impacts of climate change on the urban environment, *Current Opinion in Environmental Sustainability* 3 (3) (2011) 150–157, doi:[10.1016/j.cosust.2010.12.009](https://doi.org/10.1016/j.cosust.2010.12.009).
- [3] UN (United Nations), Transforming our world: the 2030 Agenda for Sustainable Development, A/RES/70/L.1., New York, 2015.
- [4] European Commission, *Roadmap for moving to a low-carbon economy in 2050*, Off. J. Eur. Union, Brussels, Belgium, 2011.
- [5] R. Woodhead, P. Stephenson, D. Morrey, Digital construction: from point solutions to IoT ecosystem, *Autom. Constr.* 93 (2018) 35–46, doi:[10.1016/j.autcon.2018.05.004](https://doi.org/10.1016/j.autcon.2018.05.004).
- [6] A. Ciliberti, S.M. Ventura, M. Paneroni, Implementation of an interoperable process to optimise design and construction phases of a residential building: a bim pilot project, *Autom. Constr.* 71 (2016) 62–73, The Special Issue of 32nd International Symposium on Automation and Robotics in Construction, doi:[10.1016/j.autcon.2016.03.005](https://doi.org/10.1016/j.autcon.2016.03.005).
- [7] R. Ibrahim, F.P. Rahimian, Comparison of CAD and manual sketching tools for teaching architectural design, *Autom. Constr.* 19 (8) (2010) 978–987 ISSN 0926-5805, doi:[10.1016/j.autcon.2010.09.003](https://doi.org/10.1016/j.autcon.2010.09.003).
- [8] A. Mahalingam, R. Kashyap, C. Mahajan, An evaluation of the applicability of 4d cad on construction projects, *Autom. Constr.* 19 (2) (2010) 148–159, doi:[10.1016/j.autcon.2009.11.015](https://doi.org/10.1016/j.autcon.2009.11.015).
- [9] N.M. Alves, P.J. Brtolo, Integrated computational tools for virtual and physical automatic construction, *Autom. Constr.* 15 (3) (2006) 257–271, doi:[10.1016/j.autcon.2005.05.007](https://doi.org/10.1016/j.autcon.2005.05.007).
- [10] A. Schlueter, F. Thesseling, Building information model based energy/exergy performance assessment in early design stages, *Autom. Constr.* 18 (2) (2009) 153–163, doi:[10.1016/j.autcon.2008.07.003](https://doi.org/10.1016/j.autcon.2008.07.003).
- [11] T. Bock, The future of construction automation: technological disruption and the upcoming ubiquity of robotics, *Autom. Constr.* 59 (2015) 113–121, doi:[10.1016/j.autcon.2015.07.022](https://doi.org/10.1016/j.autcon.2015.07.022).
- [12] G. Lydon, J. Hofer, B. Svetozarevic, Z. Nagy, A. Schlueter, Coupling energy systems with lightweight structures for a net plus energy building, *Appl. Energy* 189 (2017) 310–326, doi:[10.1016/j.apenergy.2016.11.110](https://doi.org/10.1016/j.apenergy.2016.11.110).
- [13] Y.-C. Yoon, K.-H. Kim, S.-H. Lee, D. Yeo, Sustainable design for reinforced concrete columns through embodied energy and CO<sub>2</sub> emission optimization, *Energy and Buildings* 174 (2018) 44–53, doi:[10.1016/j.enbuild.2018.06.013](https://doi.org/10.1016/j.enbuild.2018.06.013).
- [14] G. Lydon, J. Hofer, Z. Nagy, A. Schlueter, Thermal analysis of a multifunctional floor element, in: *Proceedings of the Third IBSPA Building Simulation Optimisation*, Newcastle, England, 2016.
- [15] G. Lydon, J. Hischier I. Hofer, A. Schlueter, High-resolution analysis for the development of tabs in lightweight structures, in: *Proceedings of the IBSPA Building Simulation*, San Francisco, USA, 2017.
- [16] B. Schleich, N. Anwer, L. Mathieu, S. Wartzack, Shaping the digital twin for design and production engineering, *CIRP Ann.* 66 (1) (2017) 141–144, doi:[10.1016/j.cirp.2017.04.040](https://doi.org/10.1016/j.cirp.2017.04.040).
- [17] A. Liew, Y. Strz, S. Guillaume, T.V. Mele, R. Smith, P. Block, Active control of a rod-net formwork system prototype, *Autom. Constr.* 96 (2018) 128–140, doi:[10.1016/j.autcon.2018.09.002](https://doi.org/10.1016/j.autcon.2018.09.002).
- [18] European Commission, *Energy Performance of Buildings Directive (recast) 2010/31/EU (EPBD)*, European Parliament, 2010.
- [19] M.K. Dixit, Life cycle embodied energy analysis of residential buildings: a review of literature to investigate embodied energy parameters, *Renew. Sustain. Energy Rev.* 79 (2017) 390–413, doi:[10.1016/j.rser.2017.05.051](https://doi.org/10.1016/j.rser.2017.05.051).
- [20] I. Sartori, A. Hestnes, Energy use in the life cycle of conventional and low-energy buildings: a review article, *Energy Build.* 39 (3) (2007) 249–257.
- [21] J. Bastos, S.A. Batterman, F. Freire, Life-cycle energy and greenhouse gas analysis of three building types in a residential area in lisbon, *Energy Build.* 69 (2014) 344–353, doi:[10.1016/j.enbuild.2013.11.010](https://doi.org/10.1016/j.enbuild.2013.11.010).
- [22] W.G. Reed, E.B. Gordon, Integrated design and building process: what research and methodologies are needed? *Build. Res. Inf.* 28 (5–6) (2000) 325–337, doi:[10.1080/096132100418483](https://doi.org/10.1080/096132100418483).
- [23] J. Nässén, F. Sprei, J. Holmberg, Stagnating energy efficiency in the swedish building sectoreconomic and organisational explanations, *Energy Policy* 36 (10) (2008) 3814–3822.
- [24] L. Walker, J. Hofer, A. Schlueter, High-resolution, parametric BIPV and electrical systems modeling and design, *Appl. Energy* 238 (2019) 164–179, doi:[10.1016/j.apenergy.2018.12.088](https://doi.org/10.1016/j.apenergy.2018.12.088).
- [25] G. Lydon, A. Willmann, J. Hofer, Z. Nagy, A. Schlueter, Balancing operational and embodied emissions for the energy concept of an experimental research and living unit, in: *Proceedings of the CISBAT*, Lausanne, Switzerland, 2015.
- [26] R. Owen, R. Amor, M. Palmer, J. Dickinson, C.B. Tatum, A.S. Kazi, M. Prins, A. Kiviniemi, B. East, Challenges for integrated design and delivery solutions, *Archit. Eng. Des. Manag.* 6 (4) (2010) 232–240, doi:[10.3763/aedm.2010.IDDS1](https://doi.org/10.3763/aedm.2010.IDDS1).
- [27] Ansys Inc, *Fluent 17.0 Theory Guide*, SAS IP, Inc, Canonsburg, U.S.A., 2016.
- [28] H. Hens, *Building Physics Heat, Air and Moisture*, Wilhelm Ernst Sohn, Berlin, 2012.
- [29] Swiss Society of Engineers & Architects (SIA), *SIA 381 Thermische Energie im Hochbau*, SIA, Zurich, Switzerland, 2016.
- [30] D. Veenendaal, J. Bakker, P. Block, Structural design of the flexibly formed, mesh-reinforced concrete sandwich shell roof of nest HiLo, *J. Int. Assoc. Shell Spat. Struct.* 58 (1) (2017) 23–38, doi:[10.20898/j.iass.2017.191.847](https://doi.org/10.20898/j.iass.2017.191.847).
- [31] T.E. Dyson, D.G. Bogard, S.D. Bradshaw, Evaluation of CFD simulations of film cooling performance on a turbine vane including conjugate heat transfer effects, *Int. J. Heat Fluid Flow* 50 (2014) 279–286, doi:[10.1016/j.ijheatfluidflow.2014.08.010](https://doi.org/10.1016/j.ijheatfluidflow.2014.08.010).

- [32] G. Augenbroe, Trends in building simulation, *Build. Environ.* 37 (2002) 891–902.
- [33] J. Andress, R. Linn, Chapter 1 - introduction to command shell scripting, in: J. Andress, R. Linn (Eds.), *Coding for Penetration Testers*, Syngress, Boston, 2012, pp. 1–33.
- [34] W. McKinney, The Pandas website, 2018, <https://pandas.pydata.org/>. Accessed: 2018-09-10.
- [35] S. de Wit, G. Augenbroe, Analysis of uncertainty in building design evaluations and its implications, *Energy Build.* 34 (9) (2002) 951–958. A View of Energy and Building Performance Simulation at the start of the third millennium.
- [36] Y. Shahtaheri, C. Rausch, J. West, C. Haas, M. Nahangi, Managing risk in modular construction using dimensional and geometric tolerance strategies, *Autom. Constr.* 83 (2017) 303–315.
- [37] T.V. Mele, A. Liew, T. Mendz, M. Rippmann, et al., COMPAS: A framework for computational research in architecture and structures., 2017, <http://compas-dev.github.io/>.
- [38] Rhinoceros 3d v5., 2016, URL <https://www.rhino3d.com/>.
- [39] D. Rutten, Grasshopper - Algorithmic Modelling for Rhino, 2018, <http://www.grasshopper3d.com/>. Accessed: 2018-09-10.
- [40] Lesosai, The Lesosai website, 2015, <http://www.lesosai.com/en/index.cfm>. Accessed: 2015-09-21.
- [41] D. Coakley, P. Raftery, M. Keane, A review of methods to match building energy simulation models to measured data, *Renew. Sustain. Energy Rev.* 37 (2014) 123–141, doi:[10.1016/j.rser.2014.05.007](https://doi.org/10.1016/j.rser.2014.05.007).
- [42] I.T. Michailidis, S. Baldi, M.F. Pichler, E.B. Kosmatopoulos, J.R. Santiago, Proactive control for solar energy exploitation: a german high-inertia building case study, *Appl. Energy* 155 (2015) 409–420, doi:[10.1016/j.apenergy.2015.06.033](https://doi.org/10.1016/j.apenergy.2015.06.033).
- [43] M. Gwerder, B. Lehmann, J. Tödtli, V. Dorer, F. Renggli, Control of thermally-activated building systems (tabs), *Appl. Energy* 85 (7) (2008) 565–581, doi:[10.1016/j.apenergy.2007.08.001](https://doi.org/10.1016/j.apenergy.2007.08.001).
- [44] D. Weber, *Modelling building thermal systems to investigate energy and comfort dependent control strategies*, ETH Zurich, 2018. Master thesis
- [45] K. Vringer, M. van Middelkoop, N. Hoogervorst, Saving energy is not easy: an impact assessment of dutch policy to reduce the energy requirements of buildings, *Energy Policy* 93 (2016) 23–32, doi:[10.1016/j.enpol.2016.02.047](https://doi.org/10.1016/j.enpol.2016.02.047).
- [46] M. Ryghaug, K.H. Sorensen, How energy efficiency fails in the building industry, *Energy Policy* 37 (3) (2009) 984–991.
- [47] M. Waskom, The Seaborn website, 2018, <https://seaborn.pydata.org/>. Accessed: 2018-09-10.